Symmetry and location of Rare Earth ions in transparent nano-glass ceramics

The aim of this proposal was to complete the structural characterisation of transparent nano-glass-ceramics, confirming the presence of doping rare earth ions in fluoride nano-crystals and to elucidate the mechanism of their inclusion into the crystalline network, through XANES and EXAFS. This information was essential for optimising the optical behaviour of these materials in photonic devices.

Scientific background

Rare earths (RE) doped materials are receiving a great attention for their wide field of applications: optics, optoelectronics and photonics. Nowadays, materials used for this purpose are fluorophosphate glasses and fluoride crystals. The former are quite unstable, difficult to produce and with a high phonon energy. Although fluoride crystals posses a very low phonon energy (≈ 300 cm^{-1}), they are expensive and mainly fabricated in Japan and China, without producers in the European market.

Oxifluoride glass-ceramics combine the transparency and mechanical and chemical resistance of the aluminosilicate glasses with the feasible RE ions incorporation and low phonon energy of the fluoride crystals, being good candidates for *up-conversion* devices. The location of RE ions in the crystalline phase enhances the laser emission intensity, essential to obtain the desired optical properties. Transparency is achieved when the crystal size is below 40 nm, avoiding light scattering. Therefore, a strict control of nucleation and crystal growth processes is necessary through a deep knowledge of the crystallisation mechanisms. We have developed LaF$_3$ glass-ceramics in the frame of the 6FP project INTERCONY that will be continued by INTERCOMAS ITN European network.

RE doped alumosilicate glasses were treated at temperatures close to the glass transition temperature, T$_g$, provoking the precipitation of fluoride crystals: LaF$_3$, NaLaF$_4$ and KLaF$_4$ [1-3]. Crystallisation mechanisms have been studied through DSC, DTA and XRD. Crystal size around 20 nm was confirmed by XRD and TEM (Fig.1). Structural characterisation has been developed mainly from ^{19}F, ^{23}Na, ^{27}Al NMR spectroscopy [4] (Figure 2), but this technique is not useful to characterise RE ions like Tm^{3+}, Eu^{3+} or Yb^{3+}. We have confirmed the presence of RE ions in the fluoride crystals through linear emission spectra and luminescence decay curves, and also their effect in the enhanced efficiency in *up-conversion* processes (Figure 3 a, b, c). However, the precise distribution of RE doping ions between glassy matrix and crystals remains as an open question, being crucial to elucidate the role of RE ions in the crystallisation process. Another key issue is to clarify the symmetry of different RE ions in La^{3+} sites and to establish their neighbouring atoms. These features are crucial to control the material processing to optimise their optical behaviour. In particular, the blue emission of the Tm^{3+}/Yb^{3+} co-doped materials can be applied in the generation of devices for high optical density storage and biomedical diagnostics.
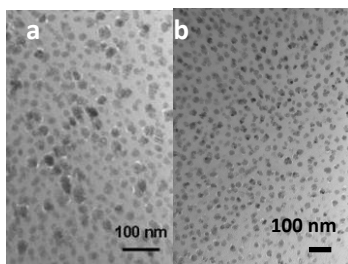

Fig.1. TEM micrographs of 55Si10La glass-ceramic a) doped with 1% mol Tm$_2$O$_3$ and b) doped with 0.5% mol Eu$_2$O$_3$
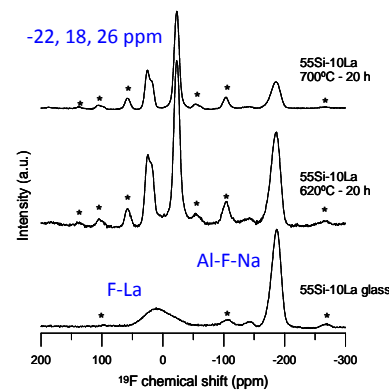
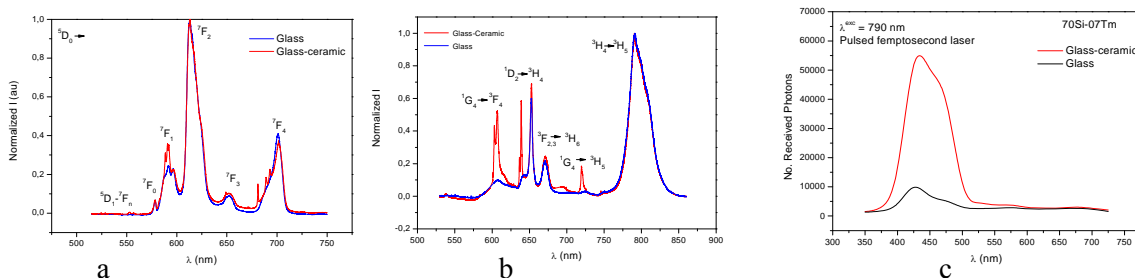Fig. 2. ^{19}F NMR spectra of 55Si10La glass and glass-ceramics

Fig.3. Emission spectra at 488 nm excitation of the (a) 55Si10La doped with 0.5% mol Eu$_2$O$_3$ and (b) 70Si7La doped with 0.7 % mol Tm$_2$O$_3$, (c) Up-conversion spectra of the 70Si7La glass and glass-ceramic.doped with 0.7% mol Tm$_2$O$_3$

Experimental technique(s), required set-up(s) and measurement strategy

Three glass compositions in the system SiO_2-Al_2O_3-Na_2O-K_2O-LaF_3 were studied, in which three different crystalline phases precipitate: LaF_3, $NaLaF_4$ and $KLaF_4$. Three optically active lanthanide ions, Tm^{3+}, Eu^{3+} and Yb^{3+}, were used for single doping and co-doping. These materials have been characterised by DSC, XRD, TEM, NMR, refractive index, absorption and emission spectroscopy, including *up-conversion* emission, and excited states lifetime measurements.

The samples were glasses and GC´s obtained varying the temperature and time of heat treatments between 540 and 620ºC, and from 20 to 150 h, respectively. Five compositions will be prepared, in which LaF_3:Tm^{3+}, LaF_3:Eu^{3+}, $NaLaF_4$:Tm^{3+}, $KLaF_4$:Eu^{3+}/Yb^{3+}, $KLaF_4$:Tm^{3+}/Yb^{3+}, nanocrystals precipitate. The original glass plus 3 GC´s obtained at different times will be measured completing a total of 20 samples. Bulk samples with 1x10x10 mm^3 and references of metallic RE ions and their oxides will be used.

Room temperature XANES and EXAFS spectra will be recorded at the Eu, Tm and Yb L_3 edges (6980, 8649 and 8944 eV respectively) in fluorescence mode. The samples will be placed in the beam path at 45º incidence angle.

Considering the energy of the Tm (8649 eV) Eu (6980 eV) and Yb (8944 eV) edges the requirement of a fluorescence detector with sensitivity for small signals, the BM25 beamline seemed the most suitable to carry out the experiments. In order to determine slight differences in the environment of the RE ions, 4 spectra will be recorded to improve the signal to noise ratio.

We expect to determine the crystalline sites of the doping RE ions in LaF_3, $NaLaF_4$ and $KLaF_4$ crystals as a function of temperature and time of the crystallising treatment, to clarify the incorporation kinetics and the preferential crystalline sites as well as the RE neighbours. This information is crucial to control the crystallising process and to optimise the optical properties of the materials.

Results and discussion

The environment of different lanthanide ions in oxyfluoride glasses and glass-ceramics in the system SiO_2-Al_2O_3-Na_2O-K_2O-LaF_3/YF_3/LuF_3 has been studied, through XANES and EXAFS.

Ionization edge L_3 was used for study the following lanthanide ions: La^{3+}, Tm^{3+}, Eu^{3+}, Er^{3+}, Yb^{3+} and Lu^{3+}, under fluorescence and transmission conditions.

Four different lanthanide doped compositions were analysed, in which different crystalline phases precipitate: LaF_3:Tm^{3+}, LaF_3:Eu^{3+}, $NaLaF_4$:Tm^{3+}, $NaYF_4$:Er^{3+}/Yb^{3+} and $LiLuF_4$:Nd^{3+}/Er^{3+}.

The ionization energy E_0 of the lanthanide ions (Ln^{3+}) was calculated from the derivate function of the XANES spectra (Figure 4). E_0 increases with the crystallisation process, from the glass to the glass-ceramics, indicating that part of the Ln^{3+} ions are distributed in a fluorine enriched environment in the glass-ceramics, instead of the oxygen one in the glass, since the electronegativity of fluorine is higher than that of oxygen. The obtained E_0 values have been compared with those of the corresponding references compounds, like TmF_3, Tm_2O_3, LaF_3, La_2O_3, LuF_3, Eu_2O_3, ErF_3, YbF_3, Yb_2O_3.
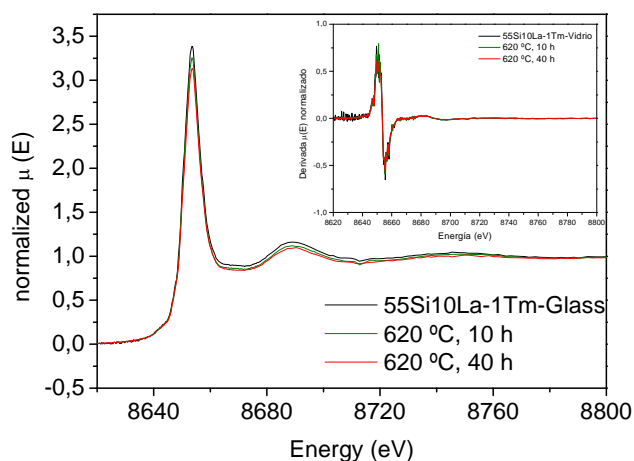

Figure 4: Tm- L_3 edge XANES spectra of a LaF_3-containing glass and glass-ceramics. Derivate function is shown in the inset.

The width of the L_3-edge varies inversely with the crystallinity of the environment. As an example, Table 1 shows a decrease of the L_3-edge width the crystallisation process, confirming that Tm^{3+} ions are located in an environment of higher crystallinity in the glass-ceramics respect to that of the glass.

Both results support an inclusion of lanthanide ions in the crystalline phase of the glass-ceramics, instead of remaining in the glassy matrix.

Table 1: E_0 of a LaF$_3$-containing glass and glass-ceramics from XANES spectra

	55Si10La-1Tm Glass	620ºC-10 h	620ºC-40 h
E_0 (eV)	8649,56	8650,91	8651,68
L_3-edge width (Lorenz function)	5,289	5,184	5,001

Figure 5 shows the $\chi(k)$ functions of a LaF$_3$-containing glass and glass-ceramics and references compounds. Fourier transformation (FT) of the $\chi(k)$-k^2 function in the k range 1 to 6 $Å^{-1}$ leads to the radial function $\chi(R)$-k^2, shown in Figure 6. Table 2 shows the distances R to the Tm nearest neighbour.
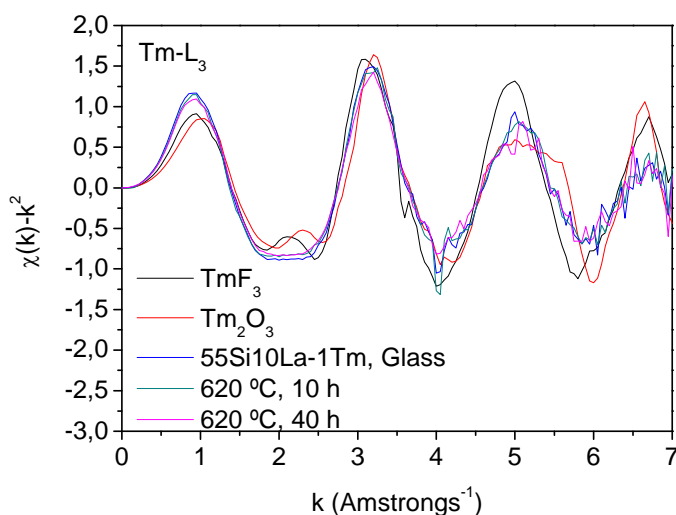

Figure 5: $\chi(k)$ functions of Tm^{3+} in LaF$_3$-containing glass and glass-ceramics and references
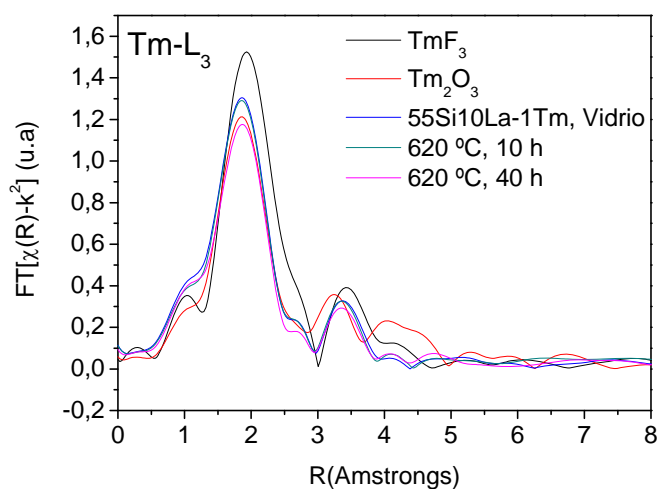

Figure 3: Radial function of Tm^{3+} in LaF$_3$-containing glass and glass-ceramics and references

Table 2: Nearest neighbour distance of Tm^{3+} in a LaF$_3$-containing glass and glass-ceramics, and references compounds

Tm-L$_3$	55Si10La-1Tm Glass	620ºC-10 h	620ºC-40 h	TmF$_3$	Tm$_2$O$_3$	LaF$_3$ (La-L$_3$)
R (Å)	1,87	1,87	1,87	1,93	1,87	2,05

The radial function of Tm^{3+} in the glass and glass-ceramics clearly shows two contributions: Within the short range order (low R values), an oxide environment dominates, since the radial functions of the glass and glass-ceramics are very similar to that of Tm$_2$O$_3$ until 3 Å. Note, that the distances R in Table 2 is 1.87 Å in the glass, glass-ceramics and Tm$_2$O$_3$.

The second contribution appears at long range order, where the radial function of the glass and glass-ceramics has the same structure than that of the TmF$_3$, being very different to that of Tm$_2$O$_3$. Thus, Tm^{3+} ions in oxygen environments do not possess long range order, and a well defined structure is not present beyond the nearest neighbour of Tm. On the contrary, fluorine environment of Tm presents long range order. In the glass, this fluorine environment are attributed to La-F phase separation regions already present in the parent glass, acting as precursors of the fluoride crystals (LaF$_3$). In the glass-ceramics, this is an evidence of the location of Tm ions in LaF$_3$ nano-crystals.

These results are representative of all the studied compositions. Taking into account the goals of the initial proposal we can confirm the objectives were successfully achieved.